

## Secondary Deuterium Isotope Effects for Enolization Reactions

William C. Alston II,<sup>‡</sup> Kari Haley, Ryszard Kanski,<sup>§</sup> Christopher J. Murray,<sup>\*,†</sup> and Julianto Pranata\*

Contribution from the Department of Chemistry and Biochemistry, University of Arkansas, Fayetteville, Arkansas 72701

Received June 27, 1994. Revised Manuscript Received November 28, 1995<sup>⊗</sup>

**Abstract:** Secondary  $\alpha$ - and  $\beta$ -deuterium isotope effects for enolization reactions and equilibria have been determined by ab initio calculations,  $^1\text{H}$  NMR spectroscopy, and triton exchange kinetics. Kinetic and equilibrium  $\alpha$ -deuterium isotope effects for hydroxide ion-catalyzed enolization of acetaldehyde calculated by ab initio methods are normal and depend on the orientation of the secondary hydrogen with respect to the carbonyl group. The computed transition state structure indicates a small degree of bond rehybridization at the transition state. Experimentally measured secondary isotope effects on the deuterioxide ion-catalyzed proton exchange of acetophenone are  $k^{\text{H}}/k^{\text{D}} = 1.08 \pm 0.07$  for  $\alpha\text{-CH}_3$  exchange and  $k^{\text{H}}/k^{\text{D}} = 0.96 \pm 0.08$  for  $\alpha\text{-CH}_2\text{D}$  exchange. For  $\alpha\text{-CH}_2\text{T}$  exchange in water, the corresponding secondary isotope effect is  $k^{\text{H}}/k^{\text{D}} = 1.06 \pm 0.02$ , assuming the rule of the geometric mean is valid. These effects are smaller than the calculated equilibrium isotope effect for formation of the enolate ion–water complex:  $K^{\text{H}}/K^{\text{D}} = 1.11\text{--}1.22$  at the MP2 level. The normal kinetic isotope effects are smaller than might be expected due to a loss in hyperconjugation of the out-of-plane C–H bond and a lag in structural reorganization that contributes to the intrinsic barrier for proton transfer from carbon. Ionization of protonated acetone gives rise to an inverse secondary isotope effect of 0.97/D for the C–L bond adjacent to the carbonyl group and is consistent with a loss in hyperconjugation upon formation of the neutral ketone.

### Introduction

Proton transfers from carbon acids activated by the carbonyl group generate enolate or enol intermediates in enzyme reactions.<sup>1</sup> Estimates of the lifetimes of enzyme-bound enolate intermediates suggest that enzymes stabilize these intermediates or avoid their formation through concerted reactions.<sup>2</sup> Secondary isotope effects can provide useful probes of the intermediacy of enol(ate)s in enzyme reactions,<sup>3,4</sup> but in order to interpret these effects accurate measures of the magnitude of secondary kinetic (KIE) and equilibrium (EIE) isotope effects for simple enolization reactions in solution are required.

Such kinetic<sup>5</sup> and equilibrium<sup>6</sup> effects have been measured, but in some cases interpretation of the data is difficult due to uncertainties associated with the experimental technique.<sup>7</sup>  $^1\text{H}$  NMR spectroscopy provides a useful method for measuring structure–reactivity effects in proton transfer reactions of carbon acids,<sup>8–10</sup> and if separate signals of the isotopic species (CHH vs CHD) can be measured simultaneously in the same sample, secondary deuterium isotope effects can be measured.<sup>11,12</sup> Computations of kinetic isotope effects using vibrational frequencies obtained from ab initio calculations can also provide useful insights into the interpretation of secondary KIEs.<sup>13</sup>

We report here secondary  $\alpha$ - and  $\beta$ -deuterium isotope effects for enolization reactions and equilibria as shown in Scheme 1,

<sup>‡</sup> Present address: Department of Biochemistry and Biophysics, Texas A&M University, College Station, TX 77843.

<sup>§</sup> Present address: Department of Chemistry, Radiochemistry and Radiation Chemistry Laboratory, Warsaw University, Al. Zwirki i Wigury 101, 02-089 Warsaw, Poland.

<sup>†</sup> Address correspondence to this author at Genencor International, Inc. 925 Page Mill Rd., Palo Alto, CA 94304.

<sup>⊗</sup> Abstract published in *Advance ACS Abstracts*, July 1, 1996.

(1) (a) Rose, I. A. *Meth. Enzymol.* **1982**, *87*, 84–97. (b) Richard, J. P. In *The Chemistry of Enols*; Rappoport, Z., Ed.; John Wiley and Sons: Chichester, 1990; Chapter 11. (c) Keeffe, J. R.; Kresge, A. J. In *The Chemistry of Enols*; Rappoport, Z., Ed.; John Wiley and Sons: Chichester, 1990; Chapter 7.

(2) (a) Thibblin, A.; Jencks, W. P. *J. Am. Chem. Soc.* **1979**, *101*, 4963–4973. (b) Gerlt, J. A.; Gassman, P. G. *J. Am. Chem. Soc.* **1992**, *114*, 5928–5934. (c) Gerlt, J. A.; Gassman, P. G. *Biochemistry* **1993**, *32*, 11943–11952. (d) Cleland, W. W.; Kreevoy, M. M. *Science* **1994**, *264*, 1887–1890. (e) Alagona, G.; Chio, C.; Kollman, P. A. *J. Am. Chem. Soc.* **1995**, *117*, 9855–9862.

(3) (a) Rose, I. A. In *Isotope Effects on Enzyme Catalyzed Reactions*; Cleland, W. W., O'Leary, M. H., Northrop, D. B., Eds.; University Park Press: Baltimore, 1977; pp 209–232. (b) Cleland, W. W. In *Isotopes in Organic Chemistry*; Buncl, E., Lee, C. C., Eds.; Elsevier: New York, 1987; Vol. 7, Chapter 2. (c) Anderson, V. E. In *Enzyme Mechanisms from Isotope Effects*; Cook, P. F., Ed.; CRC Press: Boca Raton, FL, 1991; Chapter 16.

(4) (a) Pascal, R. A.; Walsh, C. T. *Biochemistry* **1984**, *23*, 2745–2752. (b) Bahnson, B. J.; Anderson, V. E. *Biochemistry* **1989**, *28*, 4173–4181. (c) Xue, L.; Talalay, P.; Mildvan, A. S. *Biochemistry* **1990**, *29*, 7491–7500. (d) Denu, J. M.; Fitzpatrick, P. F. *Biochemistry* **1994**, *33*, 4001–4007.

(5) (a) Emmons, W. D.; Hawthorne, M. F. *J. Am. Chem. Soc.* **1956**, *78*, 5593–5596. (b) Jones, J. R. *Trans. Faraday Soc.* **1965**, *61*, 95–99. (c) Hine, J.; Kaufmann, J. C.; Cholod, M. S. *J. Am. Chem. Soc.* **1972**, *94*, 4590–4595. (d) Kresge, A. J.; Weeks, D. P. *J. Am. Chem. Soc.* **1984**, *106*, 7140–7143. (e) Andraos, J.; Kresge, A. J.; Obratsov, P. A. *J. Phys. Org. Chem.* **1992**, *5*, 322–326.

(6) Arnett, E. M.; Cohen, T.; Bothner-By, A. A.; Bushick, R. D.; Sowinski, G. *Chem. Ind.* **1961**, 473–474.

(7) (a) Abad, G. A.; Jindal, S. P.; Tidwell, T. T. *J. Am. Chem. Soc.* **1973**, *95*, 6326–6331. (b) Chiang, Y.; Kresge, A. J.; Morimoto, H.; Williams, P. G. *J. Am. Chem. Soc.* **1992**, *114*, 3981–3982.

(8) Washabaugh, M. W.; Jencks, W. P. *J. Am. Chem. Soc.* **1989**, *111*, 683–692.

(9) Murray, C. J.; Jencks, W. P. *J. Am. Chem. Soc.* **1990**, *112*, 1880–1889.

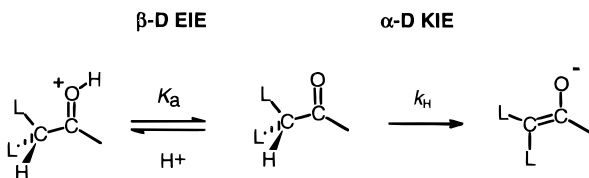
(10) Amyes, T.; Richard, J. P. *J. Am. Chem. Soc.* **1992**, *114*, 10297–10302.

(11) Jarret, R. M.; Saunders, M. *J. Am. Chem. Soc.* **1985**, *107*, 2648–2654.

(12) Perrin, C. L.; Thoburn, J. D.; Kresge, A. J. *J. Am. Chem. Soc.* **1992**, *114*, 8800–8807.

(13) (a) Saunders, M.; Laidig, K. E.; Wolfsberg, M. *J. Am. Chem. Soc.* **1989**, *111*, 8989–8994. (b) Duan, X.; Scheiner, S. *J. Am. Chem. Soc.* **1992**, *114*, 5849–5856. (c) Houk, K. N.; Gustafson, S. M.; Black, K. A. *J. Am. Chem. Soc.* **1992**, *114*, 8565. (d) Storer, J. W.; Raimondi, L.; Houk, K. N. *J. Am. Chem. Soc.* **1994**, *116*, 9675–9683. (e) Wiest, O.; Black, K. A.; Houk, K. N. *J. Am. Chem. Soc.* **1994**, *116*, 10336–10337. (f) Yoo, H. Y.; Houk, K. N. *J. Am. Chem. Soc.* **1994**, *116*, 12047–12048.

## Scheme 1



where L = H or D, using  $^1\text{H}$  NMR spectroscopy, triton exchange kinetics, and ab initio calculations.<sup>14</sup> The inverse  $\beta$ -secondary isotope effect of 0.97/D for the C–L bond adjacent to the carbonyl group in the ionization of protonated acetone is consistent with a decrease in hyperconjugation upon ionization.<sup>15,16</sup> Hyperconjugation is unchanged for the in-plane CH bond of the ketone in Scheme 1, but it is further lost in the out-of-plane CH in the enolization reaction. This gives rise to a normal secondary  $\alpha$ -deuterium KIE =  $1.06 \pm 0.02$ . Ab initio calculations suggest that the magnitude of the isotope effect is dependent on the position of the secondary CH bond relative to the carbonyl group, consistent with opposing effects of  $\text{sp}^3$ – $\text{sp}^2$  rehybridization of the OPL CH bonds and loss of hyperconjugation of the CH bonds with the carbonyl in the transition state.

## Experimental Section

**Materials.** Acetophenone- $d_3$  (99.9 atom % D), acetone- $d_5$  (99.9 atom % D), and deuterium oxide ( $\text{D}_2\text{O}$ , 99.9 atom % D) were from Isotec, Inc.  $[1\text{-}^{14}\text{C}]$ Acetophenone was from Amersham, Inc. Acetophenone and Acetophenone- $d_3$  were distilled under vacuum and stored at  $-20^\circ\text{C}$  in sealed vials. Tritiated water (TOH; 5 Ci/mL) was from ICN Biomedicals, Inc. (Costa Mesa, CA). TOH was diluted to a specific activity of 0.1 Ci/mL in  $\text{H}_2\text{O}$  or  $\text{D}_2\text{O}$ .  $[1\text{-}^3\text{H}]$ Acetophenone was synthesized by tritium exchange in TOH, giving a final specific activity of 0.273  $\mu\text{Ci}/\text{mmol}$ .  $[1\text{-}^3\text{H}, 1\text{-}^2\text{H}_2]$ Acetophenone was synthesized from acetophenone- $d_3$  in TOD (containing less than 1% HOD) to give a final specific activity of 0.123 mCi/mmol. Trimethylammonium sulfate was prepared by titrating trimethylamine with sulfuric acid, removing the water under vacuum, and drying in a vacuum oven at  $40^\circ\text{C}$  overnight. Sulfuric acid–water mixtures were prepared by dilution of commercial 98% acid and titrated with standard NaOH. All other chemicals were reagent grade and used without further purification.

**Methods.** Reactions were carried out at  $25^\circ\text{C}$ . Solution pH and pD were measured with an Orion Model 701A pH meter and a Radiometer GK2321C combination electrode. The value of pD was obtained by adding 0.4 to the observed pH of solutions in  $\text{D}_2\text{O}$ .<sup>17</sup> The optimal pD for the acetophenone  $\alpha$ -CH exchange experiments was dictated within fairly narrow limits by the buffering capacity at low deuterioxide concentrations and signal-to-noise considerations at higher base concentrations that lead to faster rates of exchange. Only solutions where the pD did not change by more than 0.02 unit were used in analysis of the data.

Proton NMR spectra were recorded on a Varian VXR-500S spectrometer in sulfuric acid/ $\text{H}_2\text{O}$  mixtures for equilibrium studies and in  $\text{D}_2\text{O}$ , 1 M ionic strength (KCl) for kinetic studies. The chemical shift of acetone and acetone- $d_5$  in sulfuric acid–water mixtures was determined by adding 1–2  $\mu\text{L}$  of acetone and 50  $\mu\text{L}$  of acetone- $d_5$  in 600  $\mu\text{L}$  of sulfuric acid/water mixtures containing 0.01 M trimethyl-

ammonium ion as an internal standard and recording the spectrum immediately after mixing with suppression of the water peak. The apparent spin–lattice relaxation times for the  $\alpha$ - $\text{CH}_3$  protons ( $T_1 = 4.5$  s), the  $\alpha$ - $\text{CH}_2\text{D}$  protons ( $T_1 = 6$  s), and the  $\alpha$ - $\text{CHD}_2$  protons ( $T_1 = 12$  s) of acetophenone were measured by the inversion recovery method ( $180^\circ - \tau - 90^\circ$ )<sup>18</sup> at 1.0 M ionic strength (KCl) in  $\text{D}_2\text{O}$ .

Experimental data were fit to eqs 1–3 using SigmaPlot (Jandel Scientific) or GraFit (Erithacus Software Ltd.).

**Acetophenone Triton Exchange in  $\text{H}_2\text{O}$ .** First-order rate constants for  $\alpha$ -C– $^3\text{H}$  exchange were determined in  $\text{H}_2\text{O}$ , ionic strength 1 M maintained with KCl by monitoring the decrease in the ratio of  $^3\text{H}$  to  $^{14}\text{C}$  in acetophenone in basic solution. Experiments with  $[1\text{-}^3\text{H}]$ -acetophenone and  $[1\text{-}^3\text{H}, 1\text{-}^2\text{H}_2]$ acetophenone were generally carried out on the same day. Radiolabeled substrate (15  $\mu\text{M}$ ;  $^3\text{H}/^{14}\text{C}$  ratio  $\approx 1.15$ ) was added in a volume of 10 mL containing 1.0 M KCl and varying amounts of KOH. Samples were quenched with HCl and frozen until HPLC separation. TOH and radiolabeled acetophenone were separated by reverse phase chromatography using a Shimadzu LC-610 system on a Shimadzu  $4 \times 250$  mm C-18 column. Samples were eluted at a flow rate of 1 mL/min with a 55:45 methanol–water mobile phase. One-milliliter fractions were collected directly into 7-mL scintillation vials, and after adding 5 mL of Opti Phase HiSafe 3 scintillation cocktail (Wallac Scintillation Products), radioactivity was determined by liquid scintillation counting on a Wallac 1410 liquid scintillation counter.

**Acetophenone Proton Exchange in  $\text{D}_2\text{O}$ .** Rate constants for  $\alpha$ -CH-exchange were determined in  $\text{D}_2\text{O}$  at  $25^\circ\text{C}$  and ionic strength 1 M maintained with KCl. Acetophenone (1  $\mu\text{L}$ ) was added to 358  $\mu\text{L}$  of deuterium oxide in a 5-mm NMR tube and sonicated followed by the addition of 375  $\mu\text{L}$  of 2.0 M KCl. The final concentration of acetophenone (ca. 10 mM) was below the limit of solubility (ca. 20 mM) in 1.0 M KCl. The magnet was carefully shimmed prior to the addition of 3–5  $\mu\text{L}$  of 0.1 M KOD to the NMR tube and reinsertion into the probe. Spectra were recorded with a digital resolution of 0.05 Hz/point and acquisition parameters were set so that the steady state  $z$  magnetization between pulses was  $\geq 95\%$  of the equilibrium magnetization of the  $\alpha$ - $\text{CHD}_2$  signal corresponding to the longest  $T_1$ .<sup>18</sup>

**Data Analysis.** For the equilibrium data, the chemical shift differences of the methyl singlet of acetone and the methyl quintet of acetone- $d_5$ , relative to trimethylammonium ion, were fit to the equations derived by Bagno et al.<sup>19</sup> that describe the equilibria in Scheme 2. The method requires estimates of limiting values of the chemical shifts  $\Delta\nu_B$ ,  $\Delta\nu_{\text{BCH}^+}$ , and  $\Delta\nu_{\text{BH}^+}$  corresponding to the free base, hydrogen-bonded complex, and protonated base, respectively, as well as values of  $m_i^*$ ,  $m^*$ ,  $pK_{\text{BCH}^+}$ , and  $pK_{\text{BH}^+}$  that define the protonation equilibria in Scheme 2. The chemical shifts are nonlinearly related so they were optimized first by minimizing the sum of the squares of the errors, then the  $m^*$  and  $pK$  values, which are linearly related, were optimized. The fitting procedure used the acidity function summarized in Bagno et al.<sup>19d</sup>

For the kinetic data, the experimental data were fit to Lorentzian line shapes using the spectrum deconvolution subroutines of VNMR.<sup>20</sup> The statistically corrected integrated areas of the  $\alpha$ - $\text{CH}_3$  singlet ( $P$ ), the  $\alpha$ - $\text{CH}_2\text{D}$  triplet ( $Q$ ), and the  $\alpha$ - $\text{CHD}_2$  quintet ( $R$ ) were simultaneously fit to eqs 1–3 that describe three consecutive first-order processes.<sup>21</sup>

(18) Derome, W. *Modern NMR Techniques for Chemistry Research*; Pergamon Press: Oxford, 1987; pp 168–170.

(19) (a) Bagno, A.; Lucchini, V.; Scorrano, G. *Bull. Soc. Chim. Fr.* **1987**, 563–572. (b) Bagno, A.; Lucchini, V.; Scorrano, G. *J. Phys. Chem.* **1991**, 95, 345–352. Bagno et al. have shown that the  $pK_a$  of protonated acetone can be obtained with a precision of  $\pm 0.03$  pK units. The excellent agreement between values of the fitting parameters obtained independently provides strong support for the approach of Bagno et al. We note that the observation that  $\Delta\nu$  for acetone- $d_5$  is less than for acetone at all values of  $H_0$  examined requires that  $pK^{d5} > pK^{h6}$ . (c) Bagno, A.; Lovato, G.; Scorrano, G. *J. Chem. Soc., Perkin Trans. 2* **1993**, 1091–1098. (d) Bagno, A.; Scorrano, G.; More O'Ferrall, R. A. *Rev. Chem. Intermed.* **1987**, 7, 313–352.

(20) Weiss, G. H.; Ferretti, J. A. *J. Magn. Reson.* **1983**, 55, 397–407.

(21) Bateman, H. *Proc. Cambridge Phil. Soc.* **1910**, 15, 423–427.

(14) The term “hydron” refers to the hydrogen cation ( $\text{L}^+$ ) without regard to nuclear mass. The specific names “proton” ( $^1\text{H}$ , H), “deuteron”, ( $^2\text{H}$ , D), and “triton” ( $^3\text{H}$ , T) refer to specific isotopes (Bunnett, J. F.; Jones, R. A. *Y. Pure Appl. Chem.* **1988**, 60, 1115–1116).

(15) Hogg, J. L. In *Transition States of Biochemical Processes*; Gandour, R. D., Schowen, R. L., Eds.; Plenum Press: New York, 1978; Chapter 5.

(16) Several workers, most notably Schowen, and his colleagues, have used the magnitude of  $\beta$ -deuterium isotope effects as a probe of transition state structure in nucleophilic acyl substitution reactions. (a) Kovach, I. M.; Hogg, J. L.; Raben, T.; Halbert, K.; Rodgers, J.; Schowen, R. L. *J. Am. Chem. Soc.* **1980**, 102, 1991–1999. (b) Harrison, R. K.; Stein, R. L. *Biochemistry* **1990**, 29, 1684–1689.

(17) Glasoe, P. K.; Long, F. A. *J. Phys. Chem.* **1960**, 64, 188–191.

$$P = P_0 e^{-\lambda_1 t} \quad (1)$$

$$Q = \frac{\lambda_1}{\lambda_2 - \lambda_1} P_0 e^{-\lambda_1 t} + \left( \frac{\lambda_1 P_0}{\lambda_1 - \lambda_2} + Q_0 \right) e^{-\lambda_2 t} \quad (2)$$

$$R = \frac{\lambda_1 \lambda_2 P_0}{(\lambda_2 - \lambda_1)(\lambda_3 - \lambda_1)} e^{-\lambda_1 t} + \left[ \frac{\lambda_1 \lambda_2 P_0}{(\lambda_1 - \lambda_2)(\lambda_3 - \lambda_2)} + \frac{\lambda_2 Q_0}{\lambda_3 - \lambda_2} \right] e^{-\lambda_2 t} + \left[ \frac{\lambda_1 \lambda_2 P_0}{(\lambda_1 - \lambda_3)(\lambda_2 - \lambda_3)} + \frac{\lambda_2 Q_0}{\lambda_2 - \lambda_3} + R_0 \right] e^{-\lambda_3 t} \quad (3)$$

In eqs 1–3,  $P_0$ ,  $Q_0$ , and  $R_0$  correspond to the initial peak areas, and  $\lambda_1$ ,  $\lambda_2$ , and  $\lambda_3$  are the pseudo-first-order rate constants for deuterioxide ion catalyzed exchange of the  $\alpha$ -CH<sub>3</sub>,  $\alpha$ -CH<sub>2</sub>D, and  $\alpha$ -CHD<sub>2</sub> protons, respectively. The triplet and quintet were not completely resolved at this field strength as shown in Figure 2, especially for early percent exchange. The integral for the quintet was adjusted for this effect by multiplying the area of the peak at  $-20.2$  Hz by 2.

**Ab Initio Calculations.** In order to provide a context for interpretation of the experimentally measured kinetic isotope effects, ab initio calculations were carried out on a simple model reaction of acetaldehyde with hydroxide ion. Structures relevant to the aldehyde-to-hydroxide ion hydron transfer reaction that lead to enolate formation include acetaldehyde, hydroxide ion, the aldehyde-hydroxide ion complex, the transition state, the enolate-water complex, the enolate ion, and the enol isomer of acetaldehyde. Numerous attempts to explore the reverse proton transfer from water to the enolate to form the enol-hydroxide ion complex were unsuccessful, suggesting that the enol-to-hydroxide proton transfer is a very favorable process that proceeds without a barrier. Additional calculations were also performed relating to the nucleophilic addition reaction of hydroxide to acetaldehyde.

Initial calculations were performed at the RHF/6-31+G(d) level.<sup>22</sup> Complete geometry optimizations were performed on all the structures. Transition states were located, and the intrinsic reaction coordinate method<sup>23</sup> was used to ensure that they properly connect the reactants and products; in fact, the reactant and product complexes were actually located as end points of the IRC. The stationary points were then reoptimized at the MP2/6-31+G(d) level.<sup>22</sup> Single point calculations at higher levels, up to MP4(SDTQ)/6-311++G(d,p), were then performed at the MP2-optimized geometries. The calculations were performed using the Gaussian-92 program<sup>24</sup> on a Silicon Graphics Indigo R-4000 workstation at the University of Arkansas.

Secondary KIEs for the reaction of hydroxide ion with acetaldehyde were computed from isotopic frequencies and calculated using the well-known formulas:<sup>13b,25</sup>

$$\text{KIE} = \text{MMI} \times \text{ZPE} \times \text{EXC} \times Q \quad (4)$$

where

$$\text{MMI} = \prod (v_{\text{D}}^r / v_{\text{H}}^r) \prod (v_{\text{H}}^{\ddagger} / v_{\text{D}}^{\ddagger}) \quad (5)$$

$$\text{ZPE} = \exp\left\{ \frac{h}{kT} \left[ \sum (v_{\text{H}}^r - v_{\text{D}}^r) - \sum (v_{\text{H}}^{\ddagger} - v_{\text{D}}^{\ddagger}) \right] \right\} \quad (6)$$

$$\text{EXC} = \prod \left\{ \frac{1 - \exp(-hv_{\text{H}}^r/kT)}{1 - \exp(-hv_{\text{D}}^r/kT)} \times \frac{1 - \exp(-hv_{\text{D}}^{\ddagger}/kT)}{1 - \exp(-hv_{\text{H}}^{\ddagger}/kT)} \right\} \quad (7)$$

$$Q = \left[ 1 + \frac{(hv_{\text{H}}^{\ddagger}/kT)^2}{24} \right] / \left[ 1 + \frac{(hv_{\text{D}}^{\ddagger}/kT)^2}{24} \right] \quad (8)$$

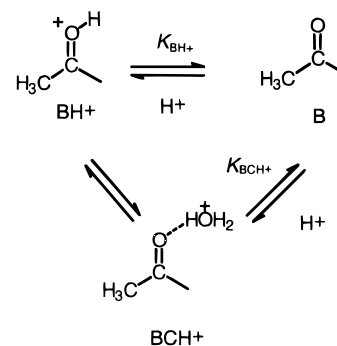
Thus, the kinetic isotope effect can be decomposed into effects due to the mass and moments of inertia (MMI), the zero point energies (ZPE),

(22) Hehre, W. J.; Radom, L.; Schleyer, P. v. R.; Pople, J. A.; *Ab Initio Molecular Orbital Theory*; Wiley Interscience: New York, 1986.

(23) (a) Gonzalez, C.; Schlegel, H. B. *J. Chem. Phys.* **1989**, *90*, 2154–2161. (b) Gonzalez, C.; Schlegel, H. B. *J. Phys. Chem.* **1990**, *94*, 5523–5527.

(24) Frisch, M. J.; Trucks, G. W.; Head-Gordon, M.; Gill, P. M. W.; Wong, M. W.; Foresman, J. B.; Johnson, B. G.; Schlegel, H. B.; Robb, M. A.; Replegle, E. S.; Gomperts, R.; Andres, J. L.; Raghavachari, K.; Binkley, J. S.; Gonzalez, C.; Martin, R. L.; Fox, D. J.; DeFrees, D. J.; Baker, J.; Stewart, J. J. P.; Pople, J. A. *Gaussian 92, Rev. B*; Gaussian, Inc.: Pittsburgh, PA, 1992.

## Scheme 2



contributions from vibrational excited states (EXC), and a tunneling correction ( $Q$ ).  $\nu_{\text{H}}^r$ ,  $\nu_{\text{D}}^r$ ,  $\nu_{\text{H}}^{\ddagger}$ , and  $\nu_{\text{D}}^{\ddagger}$  are the (real) vibrational frequencies for the hydrogen isotopomer in the reactant, the deuterium isotopomer in the reactant, the hydrogen isotopomer in the transition state, and the deuterium isotopomer in the transition state, respectively.  $\nu_{\text{H}}^i$  and  $\nu_{\text{D}}^i$  are the imaginary frequencies for the hydrogen and deuterium isotopomers in the transition state.

Equilibrium isotope effects were calculated in a similar manner,<sup>25</sup> with the vibrational frequencies of the product taking the place of the transition state; in addition, of course, the tunneling correction (eq 8) is not applicable.

Frequencies from both RHF/6-31+G(d) and MP2/6-31+G(d) calculations were used. For the KIE calculations the RHF frequencies were scaled by 0.9135, the MP2 frequencies by 0.9646.<sup>26</sup> The effects of substitution of deuterium for hydrogen at both positions of the methyl group of acetaldehyde were calculated separately (the third position is occupied by the proton being transferred, so it affects the primary, not secondary, kinetic isotope effect). The effects of a second deuterium-for-hydrogen substitution were also calculated.

Equilibrium isotope effects were also calculated for the protonation of acetone, using frequencies obtained from RHF/6-31+G(d) and MP2/6-31+G(d) calculations. The effect of a single deuterium substitution and the substitution of five deuteriums were calculated.

## Results

**$\beta$ -Deuterium Equilibrium Isotope Effects.** Bagno et al.<sup>19</sup> have shown that a complete description of the protonation equilibria of a weak base such as acetone (B, in Scheme 2) in strong acid solutions must include the formation of a hydrogen-bonded complex, BCH<sup>+</sup>, as well as the fully protonated base, BH<sup>+</sup>. Because the equilibria in Scheme 2 are established rapidly on the NMR time scale, changes in the chemical shift of the  $\alpha$ -CH resonance can be used to determine  $\text{p}K_{\text{BH}^+}$  and  $\text{p}K_{\text{BCH}^+}$ , as well as the associated  $m^*$  parameters that measure the sensitivity of the protonated species to hydrogen-bonding solvation effects.

The dependence of the chemical shift of acetone- $h_6$  and acetone- $d_5$  on the  $H_0$  acidity function<sup>19b</sup> is shown in Figure 1. The raw data are summarized in Table S1<sup>27</sup> and the fitting parameters are summarized in Table 1 along with the corresponding values determined by Bagno et al.<sup>19a</sup> for acetone. Taken together, these data yield a best estimate for  $\text{p}K_{\text{BH}^+} = -3.09 \pm 0.03$  for acetone and  $\text{p}K_{\text{BCH}^+} = -3.15 \pm 0.005$  for acetone- $d_5$ , corresponding to an isotope effect of  $K_{\text{BH}^+}^{h_6}/K_{\text{BH}^+}^{d_5} = 0.87 \pm 0.04$ .

**$\alpha$ -Deuterium Kinetic Isotope Effects.** Second-order rate constants for  $\alpha$ -C–L exchange from acetophenone catalyzed by lyoxide ion in aqueous solution were determined by detritiation<sup>8,9</sup> or <sup>1</sup>H NMR<sup>10</sup> at 25 °C and ionic strength 1.0 M

(25) (a) Bigeleisen, J.; Mayer, M. G. *J. Chem. Phys.* **1947**, *15*, 261–267. (b) Wigner, E. Z. *Phys. Chem.* **1932**, *19*, 203–216.

(26) Pople, J. A.; Scott, A. P.; Wong, M. W.; Radom, L. *Isr. J. Chem.* **1993**, *33*, 345–350.

(27) See note concerning supporting information at the end of this paper.

**Table 1.** Summary of Fitting Parameters for Equilibrium Protonation of Acetone and Acetone- $d_5$ <sup>a</sup>

substrate	chemical shift difference, Hz <sup>b</sup>			hydrogen bonded complex, BCH <sup>+</sup>		protonated base, BH <sup>+</sup>	
	$\Delta\nu_B$	$\Delta\nu_{BCH^+}$	$\Delta\nu_{BH^+}$	$m_c^*$	$pK_{BCH^+}$	$m^*$	$pK_{BH^+}$
acetone- $h_6$ <sup>c</sup>	339	284	-29.4	0.40	-1.65	0.35	-3.06
acetone- $h_6$	342	283	-21.7	0.42	-1.59	0.35	-3.11
acetone- $h_6$	341	283	-25.3	0.42	-1.59	0.35	-3.09
							$-3.09 \pm 0.03^d$
acetone- $d_5$	358	286	-20.0	0.40	-1.63	0.34	-3.15
acetone- $d_5$	358	286	-17.8	0.40	-1.68	0.34	-3.14
							$-3.15 \pm 0.005^d$

<sup>a</sup> Determined at 25 °C in concentrated sulfuric acid/water mixtures by <sup>1</sup>H NMR spectroscopy. <sup>b</sup> Positive values represent upfield shifts (in Hz) from the trimethylammonium ion, at 500 MHz. <sup>c</sup> Reference 19a. Determined at 60 MHz. Chemical shift values are corrected for the difference in field strengths. <sup>d</sup> Final values are the average ( $\pm$  standard deviation) of replicate measurements.

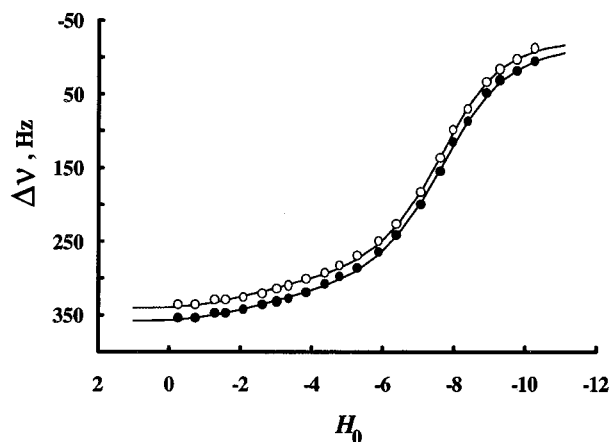


**Figure 1.** Dependence of the <sup>1</sup>H chemical shift difference between trimethylammonium ion and acetone- $h_6$  (○) or acetone- $d_5$  (●) on  $H_0$ . The theoretical curves are the best fit of the data to the model of Scheme 2 with values of  $pK_{BH} = -3.09$ ,  $m^* = 0.35$ ,  $pK_{BCH^+} = -1.59$ , and  $m_c^* = 0.42$  for acetone- $h_6$  and  $pK_{BH} = -3.14$ ,  $m^* = 0.34$ ,  $pK_{BCH^+} = -1.68$ , and  $m_c^* = 0.40$  for acetone- $d_5$ .

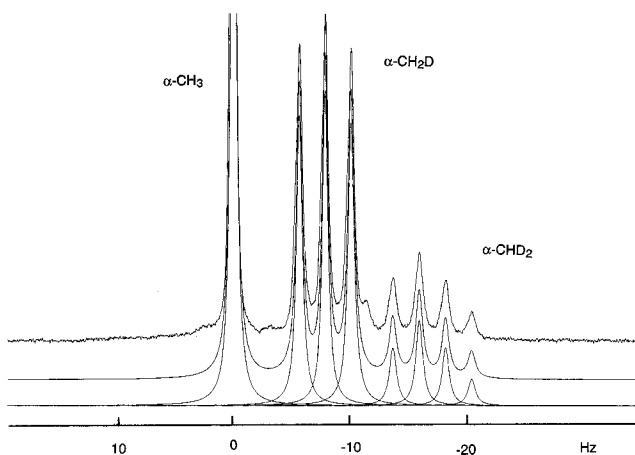


**Figure 2.** Partial 500-MHz <sup>1</sup>H NMR spectrum of the partially exchanged methyl protons of acetophenone in D<sub>2</sub>O. The top spectrum corresponds to the experimental data, the center spectrum is the full fit, and the bottom spectrum shows the individual component signals. The data were fit assuming a Lorentzian line shape.

(KCl) under pseudo-first-order conditions. Figure 2 shows representative data for  $\alpha$ -C-<sup>1</sup>H exchange monitored by <sup>1</sup>H NMR at 500 MHz indicating incomplete resolution of the multiplets for the  $\alpha$ -CH<sub>2</sub>D ( $^2J_{HD} = 2.2$  Hz) and  $\alpha$ -CHD<sub>2</sub> ( $^2J_{HD} = 2.2$  Hz) signals. The coupling constants and isotopic shifts are similar to values reported for acetone and ethylthioacetate.<sup>10</sup> In order to account for incomplete resolution, the peaks were deconvoluted assuming a Lorentzian line shape as described in the Experimental Section. Figure 3 shows a representative

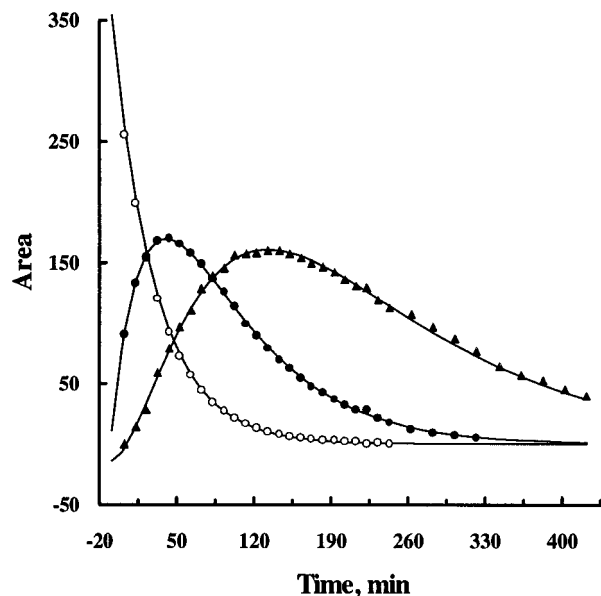
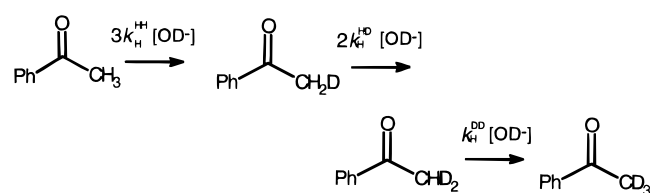


**Figure 3.** Statistically corrected areas of the  $\alpha$ -CH<sub>3</sub> (○),  $\alpha$ -CH<sub>2</sub>D (●), and  $\alpha$ -CHD<sub>2</sub> (▲) signals as a function of time for the deuteroxide ion catalyzed exchange of acetophenone in D<sub>2</sub>O at pD = 11.70 and 25 °C, ionic strength 1 M (KCl). The data were fit to the integrated rate equations describing consecutive first-order processes (Scheme 3) with rate constants  $3k_H^{HH}[\text{OD}^-] = 4.20 \times 10^{-4} \text{ s}^{-1}$ ,  $2k_H^{HD}[\text{OD}^-] = 2.52 \times 10^{-4} \text{ s}^{-1}$ , and  $k_H^{DD}[\text{OD}^-] = 1.25 \times 10^{-4} \text{ s}^{-1}$  with the corresponding secondary isotope effects  $k_H^{HH}/k_H^{HD} = 1.11$  and  $k_H^{HD}/k_H^{DD} = 1.01$ .

### Scheme 3



fit of the integrated areas as a function of time according to the mechanism of Scheme 3. The second-order rate constants for hydron exchange are defined by  $k_L^{ij}$  where L refers to the primary hydron that is cleaved and  $i$  and  $j$  refer to the remaining secondary hydron sites. The raw data are summarized in Tables S2 and S3 and the second-order rate constants and secondary KIEs calculated from the fit of the exchange data are summarized in Table 2.

Because the isotope effects are small, it is important to assess possible sources of error. The errors quoted represent replicate errors and may be subject to systematic errors. The following points suggest that the observed isotope effects are reliable. (1) The second-order rate constant for triton exchange catalyzed by hydroxide ion  $k_T^{HH} = 4.74 \pm 0.08 \times 10^{-3} \text{ M}^{-1} \text{ s}^{-1}$  is in

**Table 2.** Second-Order Rate Constants and Secondary Deuterium Isotope Effects for Lyoxide Ion Catalyzed  $\alpha$ -C–L Exchange from Acetophenone<sup>a</sup>

$\alpha$ -C–L/OL <sup>-</sup>	$10^3 k_L, \text{M}^{-1} \text{s}^{-1}$	$k_{\text{H}}^{\text{HH}}/k_{\text{H}}^{\text{HD}}$	$k_{\text{H}}^{\text{HD}}/k_{\text{H}}^{\text{DD}}$	$k_{\text{T}}^{\text{HH}}/k_{\text{T}}^{\text{DD}}$
CH <sub>3</sub> /OD <sup>-</sup>	208 ± 10	1.08 ± 0.07 <sup>b</sup>	0.96 ± 0.08 <sup>b</sup>	1.12 ± 0.04
CH <sub>2</sub> D/OD <sup>-</sup>	193 ± 9			
CHD <sub>2</sub> /OD <sup>-</sup>	201 ± 15			
CH <sub>2</sub> T/OH <sup>-</sup>	4.74 ± 0.08			
CD <sub>2</sub> T/OH <sup>-</sup>	4.22 ± 0.12			

<sup>a</sup> A 25 °C in L<sub>2</sub>O, ionic strength 1 M (KCl). <sup>b</sup> Values represent the average (± propagated error) of the ratio of second-order rate constants. The corresponding averages and standard errors based on the individual isotope effect measurements are  $k_{\text{H}}^{\text{HH}}/k_{\text{H}}^{\text{HD}} = 1.08 \pm 0.03$  and  $k_{\text{H}}^{\text{HD}}/k_{\text{H}}^{\text{DD}} = 0.96 \pm 0.06$ . The smaller errors represent cancellation of systematic errors when data are determined at the same time in the same instrument.

good agreement with  $k_{\text{T}}^{\text{HH}} = 4.7 - 5.4 \times 10^{-3} \text{M}^{-1} \text{s}^{-1}$  reported previously.<sup>28</sup> (2) For  $\alpha$ -C–<sup>1</sup>H exchange, uncertainties in the pseudo-first-order rate constants arise largely from variations in resolution set by shimming the magnet. For individual kinetic runs, the line widths did not change by more than a few hundredths of a hertz during the course of the experiments. This is consistent with the fact that the errors estimated statistically from the goodness of fit are too small to contribute to the overall observed error in the isotope effects. (3) The *simultaneous* fitting of all three data sets places severe restrictions on the quality of the data required for the fit to converge.<sup>29</sup> No restrictions on the amplitude or rate terms in eqs 1–3 were required for the fits to converge rapidly. (4) Systematic errors due to saturation effects caused by incomplete relaxation between pulses were ruled out by showing there was no change in the isotope effect when the relaxation delay times were varied from 6 to 10  $T_1$  for the  $\alpha$ -CH<sub>2</sub>D peak and 3 to 6  $T_1$  for the  $\alpha$ -CHD<sub>2</sub> peak. (5) We examined several methods of accounting for the lack of complete resolution of the multiplets including adding 0.1 Hz of line broadening, Gaussian weighting of the FIDs, and using peak heights instead of integrals.<sup>12</sup> These had no effect on the isotope effects, within the overall experimental error. (6) We examined the effect of dissolving the acetophenone in D<sub>2</sub>O, followed by the addition of KCl and doubly distilling the deuterium oxide under nitrogen to reduce dissolved carbon dioxide.<sup>30</sup> There was no change in the isotope effect, within experimental error. Finally, we note that the second-order rate constant for deuterioxide catalyzed exchange of the first  $\alpha$ -proton,  $k_{\text{H}}^{\text{HH}} = k_{\text{OD}} = 0.208 \text{M}^{-1} \text{s}^{-1}$ , when combined with a value  $k_{\text{OH}} = 0.249 \times 0.6 = 0.149 \text{M}^{-1} \text{s}^{-1}$  in H<sub>2</sub>O,<sup>31</sup> gives a solvent isotope  $k_{\text{OD}}/k_{\text{OH}} = 1.4$ , in good agreement with solvent isotope effects for enolization reactions catalyzed by lyoxide ion.<sup>32</sup>

**Calculations.** Computed energies of the stationary points for the reactions between acetaldehyde and hydroxide ion are summarized in Table 3, and Figure 4 shows relevant structures

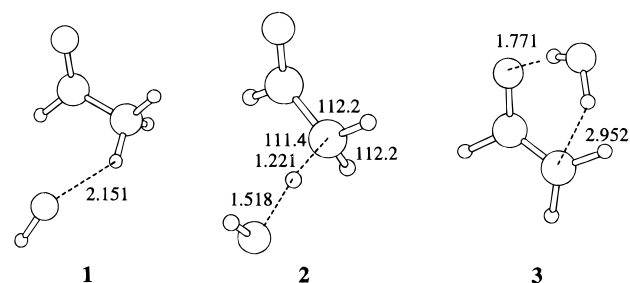
(28) (a) Jones, J. R.; Marks, R. E.; Subba Rao, S. C. *Trans. Faraday Soc.* **1967**, *63*, 111–119. (b) Jones, J. R. *Trans. Faraday Soc.* **1968**, *64*, 440–444.

(29) Ashwell, M.; Guo, X.; Sinnott, M. L. *J. Am. Chem. Soc.* **1992**, *114*, 10158–10166.

(30) Jencks, W. P.; Altura, R. A. *J. Chem. Ed.* **1988**, *65*, 770–771.

(31) (a) Chiang, Y.; Kresge, A. J.; Wirz, J. *J. Am. Chem. Soc.* **1984**, *106*, 6392–6395. (b) Calculated by correcting for the difference in the activity coefficient of hydroxide ion with ionic strength using the Debye–Hückel equation:  $-\log f_{\pm} = 0.516I^{1/2}/(1 + 1.15I^{1/2})$  at  $I = 1.0 \text{M}$ . *Lange's Handbook of Chemistry*, 14th ed.; McGraw-Hill: New York, 1992, pp 8.4 and 8.5.

(32) Casamissina, T. E.; Huskey, W. P. *J. Am. Chem. Soc.* **1993**, *115*, 14–20.

**Figure 4.** MP2-optimized structures of acetaldehyde–OH<sup>-</sup> complex (1), transition state for proton transfer (2), and enolate–H<sub>2</sub>O complex (3). Numbers shown are the O–H or C–H nonbonded distances (in angstroms) and, for 2, the bond angles of the methyl group (in degrees).

for the proton transfer reaction: the acetaldehyde–hydroxide ion complex, the transition state, and the enolate–water complex. Secondary KIEs for the enolate forming reaction are summarized in Table 4. We emphasize that these calculations do not take into account solvent effects, which undoubtedly have an important role in experimental situations. Nevertheless, trends in the experimental isotope effects are well reproduced by the calculations.

For ground state complexes qualitatively similar results are given by computations at the various levels. For example, the complexation energy is about 20 kcal/mol between the aldehyde and hydroxide ion and is slightly smaller between the enolate and water (note, however, that these values are not corrected for basis set superposition errors<sup>33</sup>). The enol tautomer of acetaldehyde is less stable than the keto tautomer by about 12–15 kcal/mol, as found previously.<sup>34</sup>

The calculated activation energy for the proton transfer reaction depends significantly on the computational level. The reaction has a significant energy barrier at the RHF level, but the barrier height is drastically reduced when electron correlation is taken into account. In fact, at the highest computational level the relative energy of the transition state is negative, i.e., the reaction does not have a barrier. It should be noted, however, that calculations at the MP3 and MP4(SDQ) level (results not shown) predict small but positive energy barriers. Overall we conclude that the energy barrier for proton transfer from acetaldehyde to hydroxide ion is quite small in the gas phase.

For the competing nucleophilic addition reaction the calculations show that the tetrahedral adduct formed is less stable than the enolate–water complex by about 5 kcal/mol and the reaction has a small energy barrier (Table 3). In this case the dependence on the computational level is not as great. This is consistent with many other examples of computations dealing with nucleophilic addition to carbonyl compounds.<sup>35</sup> It is notable that the IRC calculation from this transition state resulted in an aldehyde–hydroxide ion complex of identical structure to the one obtained in the proton transfer reaction. Also, both proton transfer and nucleophilic addition reactions have small barriers. Thus, at least for this particular system, there does not appear to be a large intrinsic preference for one reaction over the other.

For the protonation of acetone, the computed equilibrium isotope effects are summarized in Table 5. The optimized

(33) Scheiner, S. In *Reviews in Computational Chemistry*; Lipkowitz, K. B., Boyd, D. B., Eds.; VCH: New York, 1991; Vol. 2, pp 172–179.

(34) Wiberg, K. B.; Breneman, C. M.; LePage, T. J. *J. Am. Chem. Soc.* **1990**, *112*, 61.

(35) (a) Weiner, S. J.; Singh, U. C.; Kollman, P. A. *J. Am. Chem. Soc.* **1985**, *107*, 2219–2229. (b) Madura, J. D.; Jorgensen, W. L. *J. Am. Chem. Soc.* **1986**, *108*, 2517–2527. (c) Blake, J. F.; Jorgensen, W. L. *J. Am. Chem. Soc.* **1987**, *109*, 3856–3861. (d) Krug, J. P.; Popelier, P. L. A.; Bader, R. W. F. *J. Phys. Chem.* **1992**, *96*, 7604–7616. (e) Francisco, J. S.; Williams, I. H. *J. Am. Chem. Soc.* **1993**, *115*, 3746–3751. (f) Pranata, J. *J. Phys. Chem.* **1994**, *98*, 1180–1184.

**Table 3.** Relative Energies of Stationary Points along the Reaction Coordinates for Reaction of Hydroxide Ion with Acetaldehyde<sup>a</sup>

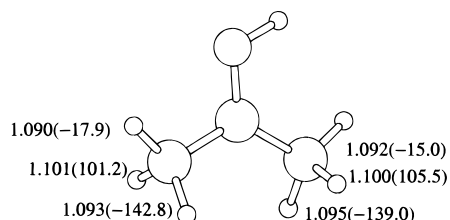
	aldehyde + OH <sup>-</sup>	aldehyde-OH <sup>-</sup> complex	transition state	enolate-H <sub>2</sub> O complex	enolate + H <sub>2</sub> O	enol + OH <sup>-</sup>	nucleophilic addition TS	nucleophilic addition product
RHF/6-31+G(d)	18.7	0	7.3	-18.1	-1.3	34.7	2.7	-13.4
MP2/6-31+G(d)	19.9	0	1.2	-17.7	2.2	35.5	1.3	-15.0
MP2/6-311++G(d,p)	19.6	0	-0.6	-22.0	-2.9	31.6	1.2	-15.0
MP4(SDTQ)/6-311++G(d,p)	20.0	0	-0.3	-20.7	-1.6	33.0	0.6	-14.7

<sup>a</sup> Energies are in kcal/mol relative to the aldehyde-OH complex, whose total energy is -228.35632, -228.97806, -229.12074, or -229.17690 au at the various computational levels listed in the table.

**Table 4.** Calculated Secondary Deuterium KIEs for Enolate Formation

	MMI	ZPE	EXC	Q	overall KIE	EIE <sup>a</sup>	EIE <sup>b</sup>
RHF Frequencies							
$k^{HH}/k^{HD}$	1.006	1.053	1.042	1.001	1.105	1.279	1.200
$k^{HH}/k^{DH}$	0.987	0.981	1.088	1.005	1.057	1.179	1.099
$k^{HD}/k^{DD}$	0.987	0.992	1.077	1.005	1.060	1.187	1.106
$k^{DH}/k^{DD}$	1.006	1.065	1.032	1.001	1.107	1.288	1.208
MP2 Frequencies							
$k^{HH}/k^{HD}$	0.986	1.024	1.036	1.004	1.050	1.324	1.214
$k^{HH}/k^{DH}$	0.970	0.960	1.071	1.004	1.002	1.224	1.103
$k^{HD}/k^{DD}$	0.970	0.971	1.062	1.004	1.005	1.231	1.111
$k^{DH}/k^{DD}$	0.986	1.036	1.027	1.003	1.053	1.332	1.222

<sup>a</sup> Calculated from frequencies of isolated acetaldehyde and enolate. <sup>b</sup> Calculated from frequencies of the aldehyde-hydroxide ion and enolate-water complexes.

**Figure 5.** MP2-optimized structure of protonated acetone. Numbers displayed are the C-H bond lengths (in angstroms) and the H-C-O dihedral angles (in degrees).

structure of protonated acetone is shown in Figure 5. Protonation causes an approximately 15–20° rotation of both methyl groups in opposite directions, thus each of the six methyl hydrogens is unique. Table 5 displays the isotope effects for substitution at each of these six positions. Acetone itself is  $C_{2v}$ -symmetric at the RHF level; however, optimization at the MP2 level resulted in a structure with  $C_2$  symmetry, with the methyl groups rotated by about 6°.

## Discussion

**The Nature of the Transition State for Base-Catalyzed Enolization.** The rate constants summarized in Table 2 lead to three separate determinations of the effect of a single  $\alpha$ -deuterium substitution on the rate of ionization of a CH bond. The isotope effects determined by <sup>1</sup>H NMR for proton exchange

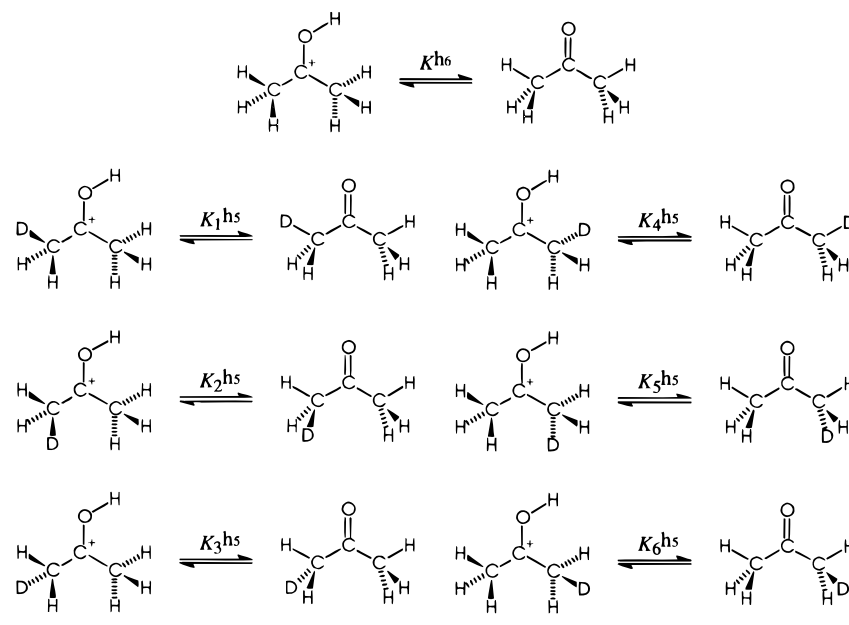
of CHH and CHD are not significantly different from one another. In the case of triton exchange, the effect of a single deuterium substitution may be given by the rule of the geometric mean:  $k_T^{HH}/k_T^{HD} = (k_T^{HH}/k_T^{DD})^{1/2} = 1.06 \pm 0.02$ . Combined with the corresponding values for proton exchange this gives a weighted average isotope effect of a single  $\alpha$ -deuterium substitution on the rate of ionization of a CH bond:  $k^H/k^D = 1.06 \pm 0.01$ .<sup>37</sup> We must however be cautious in applying the rule of the geometric mean since it implies that the effect of isotopic substitution is completely localized to the bond being substituted. Indeed, the calculated isotope effects (Table 4) indicate a much larger effect when the deuterium is syn to the carbonyl group. In any event the calculated equilibrium isotope effects in Table 4 ranging from 1.10 to 1.32 are larger than this value.

There is extensive evidence for a substantial degree of proton transfer to the base catalyst (Scheme 4) in the transition state for enolization reactions as measured by Brønsted  $\beta$  coefficients of  $\approx 0.5$ .<sup>38</sup> In addition, values of  $k_{OD}/k_{OH}$  that are intermediate between 1 and the equilibrium solvent isotope effect for the ionization of water are consistent with a proton that is half-transferred.<sup>32</sup> If rehybridization of the  $\alpha$ -carbon is synchronous with the degree of proton transfer to the base catalyst, the  $\alpha$ -secondary KIE should be intermediate between 1.0 and the average equilibrium isotope effect of 1.10–1.32 (Table 4) as is

(37) Bevington, P. R.; Robinson, D. K. In *Data Reduction and Error Analysis for the Physical Sciences*, 2nd ed.; McGraw-Hill: New York, 1992; pp 58–60.

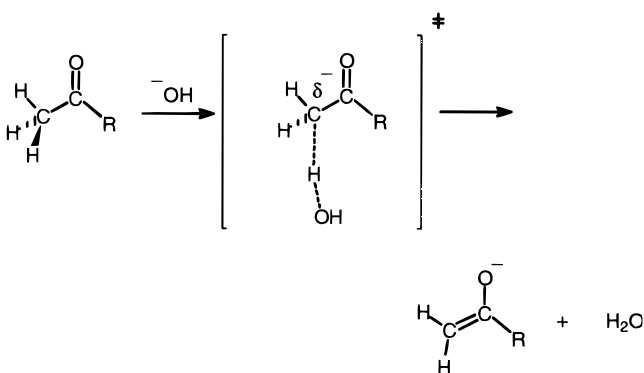
(38) (a) Bell, R. P. In *The Proton in Chemistry*, 2nd ed.; Cornell University Press: Ithaca, New York, 1973; Chapter 10. (b) Bell, R. P.; Grainger, S. *J. Chem. Soc., Perkin Trans. 2* **1976**, 1367–1370. (c) Chiang, Y.; Kresge, A. J.; Santabella, Wirz, J. *J. Am. Chem. Soc.* **1988**, *110*, 5506–5510. (d) Stefanidis, D.; Bunting, J. W. *J. Am. Chem. Soc.* **1991**, *113*, 991–995.

(36) (a) Defrees, D. J.; Taagepera, M.; Levie, B. A.; Pollack, S. K.; Summerhas, K. D.; Taft, R. W.; Wolfsberg, M.; Hehre, W. J. *J. Am. Chem. Soc.* **1979**, *101*, 5532–5536. (b) Pross, A.; Radom, L.; Riggs, N. V. *J. Am. Chem. Soc.* **1980**, *102*, 2253–2259. (c) Saunders, M.; Cline, G. W. *J. Am. Chem. Soc.* **1990**, *112*, 3955–3963.

**Table 5.** Calculated Equilibrium Isotope Effects for the Protonation of Acetone<sup>a</sup>


	MMI	ZPE	EXC	overall EIE		MMI	ZPE	EXC	overall EIE
RHF Frequencies									
$K^{h6}/K_1^{h5}$	1.026	1.026	1.000	1.020	$K^{h6}/K_1^{d5}$	0.993	1.034	0.973	1.000
$K^{h6}/K_2^{h5}$	0.999	1.089	0.979	1.066	$K^{h6}/K_2^{d5}$	0.987	0.980	0.991	0.958
$K^{h6}/K_3^{h5}$	0.999	0.936	1.006	0.940	$K^{h6}/K_3^{d5}$	0.988	1.132	0.969	1.084
$K^{h6}/K_4^{h5}$	0.994	1.013	0.998	1.005	$K^{h6}/K_4^{d5}$	0.992	1.049	0.974	1.014
$K^{h6}/K_5^{h5}$	0.999	1.061	0.983	1.042	$K^{h6}/K_5^{d5}$	0.987	1.004	0.987	0.979
$K^{h6}/K_6^{h5}$	0.999	0.955	1.001	0.955	$K^{h6}/K_6^{d5}$	0.987	1.110	0.973	1.067
MP2 Frequencies									
$K^{h6}/K_1^{h5}$	0.999	1.033	0.990	1.022	$K^{h6}/K_1^{d5}$	0.994	0.974	0.969	0.939
$K^{h6}/K_2^{h5}$	0.999	1.059	0.983	1.040	$K^{h6}/K_2^{d5}$	0.994	0.952	0.975	0.923
$K^{h6}/K_3^{h5}$	0.998	0.932	1.004	0.933	$K^{h6}/K_3^{d5}$	0.995	1.077	0.959	1.027
$K^{h6}/K_4^{h5}$	1.001	1.011	0.990	1.001	$K^{h6}/K_4^{d5}$	0.993	0.996	0.969	0.958
$K^{h6}/K_5^{h5}$	0.999	1.039	0.985	1.022	$K^{h6}/K_5^{d5}$	0.995	0.970	0.973	0.938
$K^{h6}/K_6^{h5}$	0.998	0.951	1.000	0.949	$K^{h6}/K_6^{d5}$	0.995	1.055	0.962	1.010

<sup>a</sup>  $K_n^{d5}$  is the equilibrium constant for the reaction shown for  $K_n^{h5}$  in the figures with replacement of D with H and vice versa.

**Scheme 4**

observed. However, there is also extensive evidence for a lag in structural and solvational reorganization associated with these reactions, such that rehybridization at the  $\alpha$ -carbon is expected to lag behind proton transfer.<sup>39</sup>

The computed transition state structures and KIEs summarized in Table 4 provide some insight into the origins of the small

magnitude of these isotope effects in enolization reactions. The computed KIEs are normal, qualitatively consistent with expectations for a reaction where a CH out-of-plane bending mode changes from high frequency to low as the  $sp^3$ -hybridized carbon is converted to  $sp^2$ . As shown in Figure 4, in the transition state, the three remaining substituents on the  $\alpha$ -carbon have bond angles of about  $112^\circ$  with each other, consistent with a largely tetrahedral  $sp^3$ -like structure. In addition, the MP2-optimized structure suggests an early transition state: the distance from the hydrogen atom being transferred is 1.22 Å to the carbon atom of the aldehyde and 1.52 Å to the oxygen of the hydroxide (the RHF optimized structure suggests a somewhat later transition state, the distances being 1.30 and 1.35 Å, respectively, but this would still be considered early). The computed structures provide support for the conclusion that a lag in structural reorganization is partially responsible for the large intrinsic barriers for proton transfers to and from carbon.<sup>39</sup>

The data in Table 4 show that deuterium substitution in the position *syn* to the carbonyl oxygen (corresponding to the rate constant  $k^{HD}$ ) leads to larger overall KIEs than for deuterium substitution in the out-of-plane position (corresponding to  $k^{DH}$ ). In the optimized structure of acetaldehyde, the C–H bond lengths are 1.0916 Å for the in-plane (*syn*) position and 1.0962 Å for the out-of-plane position (these are MP2-optimized values; the RHF values are 1.0818 and 1.0868 Å). The *syn* position is

(39) (a) Bernasconi, C. F. *Adv. Phys. Org. Chem.* **1992**, 27, 116–238. (b) Bernasconi, C. F.; Wentzel, P. J. *J. Am. Chem. Soc.* **1994**, 116, 5405–5413.

(40) Streitwieser, A., Jr.; Jagow, R. H.; Fahey, R. C.; Suzuki, S. *J. Am. Chem. Soc.* **1958**, 80, 2326–2332.

not affected by hyperconjugation with the carbonyl group and has a correspondingly shorter CH bond. Acetaldehyde is a textbook case of hyperconjugation: electron donation from the CH orbital of the methyl group to the  $\pi^*$  orbital of the carbonyl strengthens the C–C bond and weakens the C–H bonds. However, due to symmetry the in-plane C–H bond is not affected.

The in-plane and out-of-plane CH bond lengths become more nearly equal in the transition state with MP2 values of 1.0936 and 1.0956 Å and RHF values of 1.0863 and 1.0885 Å, respectively. This is consistent with the notion that hyperconjugation decreases in the transition state compared to the reactants. Decreased hyperconjugation means that the out-of-plane CH bond is relatively stronger in the transition state, which causes a tendency toward an inverse KIE. The net effect is a smaller normal KIE for deuterium at the out-of-plane positions (calculated to be  $k^{\text{HH}}/k^{\text{DH}} = 1.057$  (RHF) or 1.002 (MP2)). Deuterium substitution at the syn position leads to a slightly larger KIE:  $k^{\text{HH}}/k^{\text{HD}} = 1.105$  (RHF) or 1.050 (MP2). An analogous argument regarding the compensating effects of hyperconjugation and  $\text{sp}^2\text{--sp}^3$  rehybridization has been made to explain the small magnitude of secondary kinetic isotope effects observed in the ketonization of enols.<sup>41</sup>

Unfortunately, there are still ambiguities in the calculations: in the aldehyde–hydroxide ion complex, the corresponding MP2 bond lengths are 1.0950 and 1.0976 Å, and their difference is intermediate between that for isolated acetaldehyde and the transition state; however, the RHF bond lengths are 1.0864 and 1.0873 Å, the difference being *smaller* than in the transition state.

#### $\beta$ -Deuterium Isotope Effects. Protonation of Acetone.

The  $\beta$ -deuterium equilibrium isotope effect  $K_{\text{BH}^+}^{\text{H}6}/K_{\text{BH}^+}^{\text{D}5} = 0.87 \pm 0.04$  for ionization of protonated acetone is consistent with a loss of hyperconjugation upon going from protonated acetone to acetone in concentrated acid solutions. The observed isotope effect corresponds to an equilibrium isotope effect of  $(0.87)^{1/5} = 0.97$  per deuterium, if the effects of deuterium substitution are additive. This value is similar to the calculated  $\beta$ -deuterium isotope effects in Table 5 (average  $K^{\text{H}6}/K^{\text{D}5} = 0.99$  at the MP2 level) and values of 0.93–0.96 per deuterium for the equilibrium  $(\text{CL}_3)_2\text{C}^+ + \text{X}^- \rightleftharpoons (\text{CL}_3)_2\text{C}^-\text{X}$ .<sup>42</sup> These values are less inverse than the EIE for the acidity constant of protonated acetophenone,  $K_{\text{BH}^+}^{\text{H}3}/K_{\text{BH}^+}^{\text{D}3} = (0.78)^{1/3} = 0.92/\text{D}$ .<sup>6</sup> This latter value was determined using the Hammett indicator method and is subject to the experimental uncertainties associated with that technique.<sup>19</sup> Comparison of the inverse isotope effect with EIE for ketone to alcohol equilibria of 0.95/D that corresponds to complete loss of hyperconjugation<sup>43</sup> suggests that there is a small increase in hyperconjugation in protonated acetone relative to acetone.

The calculated equilibrium isotope effects for the protonation of acetone summarized in Table 5 show again that larger effects

are observed when deuterium is substituted for hydrogen at the position syn to the carbonyl oxygen. Protonation causes rotation of both methyl groups by about 15–20°, so that one hydrogen on each methyl group is in a nearly perpendicular position. These hydrogens are most subject to hyperconjugation effects, and are observed to have the longest bonds to carbon (Figure 5). In unprotonated acetone, these hydrogens are out of plane, still affected by hyperconjugation, but not as much. Thus, deuterium substitution at these position leads to an increase isotope effect ( $K^{\text{H}6}/K_3^{\text{H}5}$  and  $K^{\text{H}6}/K_6^{\text{H}5}$ ). The in-plane hydrogen in acetone ends up only slightly out of plane upon protonation, resulting in no significant change in the hyperconjugation effects, and the expected isotope effect is minimal ( $K^{\text{H}6}/K_1^{\text{H}5}$  and  $K^{\text{H}6}/K_4^{\text{H}5}$ ). The remaining hydrogen is subject to greater hyperconjugation effects in the unprotonated species, resulting in a normal isotope effect ( $K^{\text{H}6}/K_2^{\text{H}5}$  and  $K^{\text{H}6}/K_5^{\text{H}5}$ ). Thus, the changes in hyperconjugation that lead to the computed isotope effects can be attributed primarily to geometric changes, rather than any inherent electronic effects. The results shown in Table V are consistent with this analysis. The actual observed isotope effect would presumably be some weighted average of these. Since substitution at different sites results in different effects, predicting the effects of multiple deuterium substitution is not straightforward. For the  $d_5$  isotopomer, MP2 calculations appear to predict an overall small, inverse isotope effect, qualitatively in agreement with the experimental results.

**Conclusions.** The effect of secondary  $\alpha$ -deuterium substitution on the rate of ionization of a CH bond is small for enolization reactions, consistent with a loss in hyperconjugation as well as a lag in structural reorganization at the  $\alpha$ -carbon, which gives rise to a large intrinsic barrier for proton transfer from carbon. The equilibrium isotope effect of 0.97/D on the acidity constant of protonated acetone is consistent with a small increase in hyperconjugation between the  $\alpha$ -CH bond and the positively charged carbonyl group upon protonation. These isotope effects serve as limiting models for interpretation of corresponding secondary isotope effects in enzyme reactions which will be reported in further communications.

**Acknowledgment.** We gratefully acknowledge the National Institutes of Health (GM 43251) and the Petroleum Research Fund administered by the American Chemical Society for support of this work. Kari Haley was supported by a summer undergraduate research fellowship from the National Science Foundation (CHE-9200036). We thank Professors A. Bagno and James Keeffe for helpful discussions and Marvin Leister for help in obtaining the NMR spectra.

**Supporting Information Available:** Table S1 summarizing chemical shift differences of acetone and acetone- $d_5$  as a function of weight percent sulfuric acid, Tables S2 and S3 summarizing pseudo-first-order rate constants for acetophenone proton exchange in  $\text{D}_2\text{O}$  and triton exchange in  $\text{H}_2\text{O}$ , and Tables S3 and S4 summarizing RHF and MP2 optimized structures (12 pages). Ordering information is given on any current masthead page.

JA942053K

(41) Andraos, J.; Kresge, A. J.; Obratsov, P. A. *J. Phys. Org. Chem.* **1992**, 5, 322–326.

(42) Williams, I. H. *J. Chem. Soc., Chem. Commun.* **1985**, 510–511.

(43) Cook, P. F.; Blanchard, J. S.; Cleland, W. W. *Biochemistry* **1980**, 19, 4853–4858.